J Solid State Electrochem (2015) 19:2565–2577
DOI 10.1007/s10008-015-2770-6

ORIGINAL PAPER

Electrochemical and nanogravimetric studies of poly(copper phthalocyanine) microparticles immobilized on gold in aqueous solutions

Katalin Borsos · György Inzelt

Received: 25 December 2014 / Revised: 21 January 2015 / Accepted: 23 January 2015 / Published online: 8 February 2015

Abstract An electrochemical quartz crystal nanobalance has been used to study the redox behavior of poly(copper phthalocyanine) (poly(CuPc)) microparticles attached to gold. The electrodes were investigated in contact with aqueous solutions at different pH values. In acid solutions, in the pH range from 0 to 3, one pair of reduction and reoxidation waves can be detected in the potential region from 0.8 V vs. SCE to the beginning of the hydrogen evolution. Until 0.8 V, no oxidation of the poly(CuPc) sample occurs. The reduction is accompanied with a mass increase; the original mass of the surface layer is regained during reoxidation. Below pH 0, two pairs of waves appear attesting the formation of the doubly protonated poly(CuPc). A ca. −60 mV/pH dependence of the peak potentials indicates the participation of H^+ ions in the redox reactions in an 1 H^+/1 e^- ratio in acidic and neutral solutions and the formation of 1 OH^- ion/1 e^- in basic electrolytes. In neutral and alkaline solutions, however, the mass changes become more complicated. In alkaline media, during electroreduction, a mass decrease occurs in the beginning of the reduction which is followed by a mass increase. In the course of reoxidation, the opposite pattern can be detected in respect of the mass changes. The peak currents show a minimum value at neutral pH. On the other hand, the mass changes are substantially higher in alkaline solutions than in acidic ones, i.e., the apparent molar mass values that can be determined are much higher, which is related to the dimerization causing a structural change and dehydration of the layer. The redox processes can be assigned to the reduction and oxidation of the Pc ring. The mass changes are related to the sorption and desorption of counterions and solvent molecules; however, coions also enter and leave the layer. Based on these observations, redox schemes are proposed.

Keywords Poly(copper phthalocyanine) · Microparticles · Electrochemical quartz crystal nanobalance (EQCN) · Redox transformations · Structural changes

Introduction

Studies on the electrochemical behavior of phthalocyanines have been in the foreground of research during the last 30 years [1–27 and the citations therein]. Metallophthalocyanines have been investigated especially as a catalyst of the oxygen reduction reaction (ORR), since it is of utmost importance to find a suitable and cheap catalyst which could replace the expensive platinum [1, 8, 11–13, 15, 18, 19]. A wide range of other applications beside catalysis such as in electrochromic display devices [1, 3, 7, 8, 26], in electrochemical power sources including solar cells [1, 13, 21, 24], and in sensors [8, 11, 17, 20] has also been put forward. The enhancement of the conductivity of phthalocyanines has extensively been studied as well [21, 22, 24]. It was also recognized that the protonation plays an important role in the physical and chemical properties of these compounds

This paper is dedicated to Professor Mikhail A. Vorotyntsev on the occasion of his 70th birthday with the appreciation of his outstanding contribution to the development of electrochemistry.

Electronic supplementary material The online version of this article (doi:10.1007/s10008-015-2770-6) contains supplementary material, which is available to authorized users.

K. Borsos · G. Inzelt (✉)
Department of Physical Chemistry, Institute of Chemistry, Eötvös Loránd University, Pázmány Péter sétány 1/A,
1117 Budapest, Hungary
e-mail: inzeltgy@chem.elte.hu

[22, 23, 25, 27]. However, the elucidation of the electrochemical processes occurring during the redox transformations of phthalocyanines is an interesting and challenging task in itself. In the literature, very diverse cyclic voltammograms can be found even for the same metallophthalocyanine. The main reason is that the voltammetric and other (e.g., spectroscopic) responses of phthalocyanine ring (Pc) strongly depend on metal ions in the center of the ring, the substituents on the periphery of the macrocyclic ring, the solvent and the electrolyte used, the presence of oxygen, the potential range, and even the method of the deposition.

According to theoretical considerations, the redox transformation of the central metal ion can be observed in the case of CoPc and FePc, while concerning other metal phthalocyanines such as Cu, Ni, Zn, Pt, and Pd, the metal ions do not participate in redox processes, only the Pc ring will be oxidized or reduced [6, 8, 10]. A wide arsenal of non-electrochemical methods has been used to characterize the different phthalocyanines; however, the electrochemical quartz crystal nanobalance (EQCN) [27] has not been exploited, yet. Only limited studies (mostly on the electrooxidation of metal phthalocyanines) have been carried out on platinum phthalocyanine [7], palladium phthalocyanine [9, 14], and iron phthalocyanine [15]. It is evident that the results of EQCN experiments can provide different, valuable information of the electrochemical transformations of solid particles immobilized on metal surfaces [28–31]. Therefore, in the present study, we focus our attention on the EQCN study of poly(copper phthalocyanine) (poly(CuPc)) microparticles attached to gold and investigated under different conditions. We used poly(CuPc) (Fig. 1) because it can be assumed that the polymer shows the typical behavior of CuPc but has a much better conductivity. Therefore, the problem of the poor conductivity and its changes during the redox transformations can be eliminated [15]. Furthermore, the investigation of poly(copper phthalocyanine) is attractive because it is a conjugated system which may show the behavior of a conducting polymer [32].

CuPc and poly(CuPc) have been prepared and investigated for almost 80 years; however, their electrochemical characterization is scarce because its electrocatalytic activity is poor in comparison with that of other metal phthalocyanines, e.g., FePc and CoPc. Nevertheless, CuPc is famous among the phthalocyanines since it has a brilliant blue color, and it has been produced in a large amount for paints and dyes [1, 27]. Copper phthalocyanine is also an important material used in organic solar cells and organic light-emitting diodes (OLEDs) [8, 21, 22, 24–26]. CuPc at pH 7.3 between −0.9 and 0.6 V shows a featureless voltammogram [8]. Soluble copper phthalocyanine, Na-tetrasulfonate (CuPcTS), was used as a counterion during the electropolymerization of pyrrole. It was concluded that CuPcTS incorporated in the polypyrrole layer was electrochemically inactive [16].

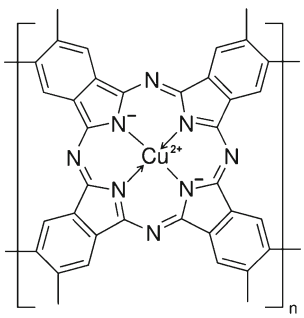

Fig. 1 The formula of poly(copper phthalocyanine)

Experimental

Poly(copper phthalocyanine) (Aldrich) was used without further purification. Analytical-grade chemicals such as $HClO_4$, $NaClO_4$, KCl (Merck), H_2SO_4, CsCl (Sigma Aldrich), K_2SO_4, Na_2SO_4, NaOH (Molar Chemicals), HCl (Riedel-de-Haën), NaCl (Chemolab), KOH, KH_2PO_4, and Na_2HPO_4 (Reanal) were used as received. Doubly distilled water was used (Millipore water). All solutions were purged with oxygen-free argon (purity 5.0, Linde Gas Hungary Co. Cltd.), and an inert gas blanket was maintained throughout the experiments.

A sodium chloride-saturated calomel electrode (SCE) was used as the reference electrode which was carefully separated from the main compartment by using a double frit. A gold wire served as the counter electrode. Poly(Cu-phthalocyanine) microparticles were immobilized on the gold surface from a poly(CuPc)-ethanol sol via dropping an adequate amount of the suspension and drying it. (Mechanical abrasion method was also used to deposit poly(CuPc) layer on EQCN electrode. Similar voltammetric and EQCN responses were obtained also for these layers; however, it was more difficult to control the amount attached to the electrode surface. Therefore, these results are not reported herein.)

Five-megahertz AT-cut crystals of 1-in. diameter coated with gold (Stanford Research Systems, SRS, USA) were used in the EQCN measurements. The electrochemically and the piezoelectrically active areas were equal to 1.37 and 0.4 cm^2, respectively.

The Sauerbrey equation [28] was used to relate the surface mass change (Δm) to the frequency shift (Δf):

$$\Delta f = -C_f \Delta m / A \quad (1)$$

The integral sensitivity of the crystals (C_f) was found to be 56.6×10^6 Hz g^{-1} cm^2, i.e., 1 Hz corresponds to 17.7 ng cm^{-2}. The integral sensitivity was calculated by using the frequency change and the charge measured during silver deposition/dissolution as well as for the electroreduction of gold oxide

in order to determine the real surface area of the electrode. The apparent molar mass of the deposited or the exchanged species (M) was calculated from the slope of the Δf vs. Q curve using the following formula:

$$M = (nFA/C_f)\mathrm{d}\Delta f/\mathrm{d}Q \quad (2)$$

where n is the number of electrons involved in the electrochemical reaction, F is the Faraday constant, Δf is the frequency change, Q is the charge consumed, and A is the electrode surface area. The capacitive charge and the frequency change originated from the free gold surface were neglected. It was checked that the effect of the free gold surface is minimal under the conditions applied in this studies. Although the requirements (uniform and homogeneous surface layer) for the application of Sauerbrey equation are not perfectly met, on the basis of measured frequency values, a rough estimation can be done. The relative values of Δf obtained for the incorporation of different ions and solvent molecules, however, should be approximately correct. The crystals were mounted in the holder made from Kynar and connected to a SRS QCM 100 unit. An Elektroflex 453 potentiostat and a Universal Frequency Counter PM6685 (Fluke) connected with an IBM personal computer were used for the control of the measurements and for the acquisition of the data.

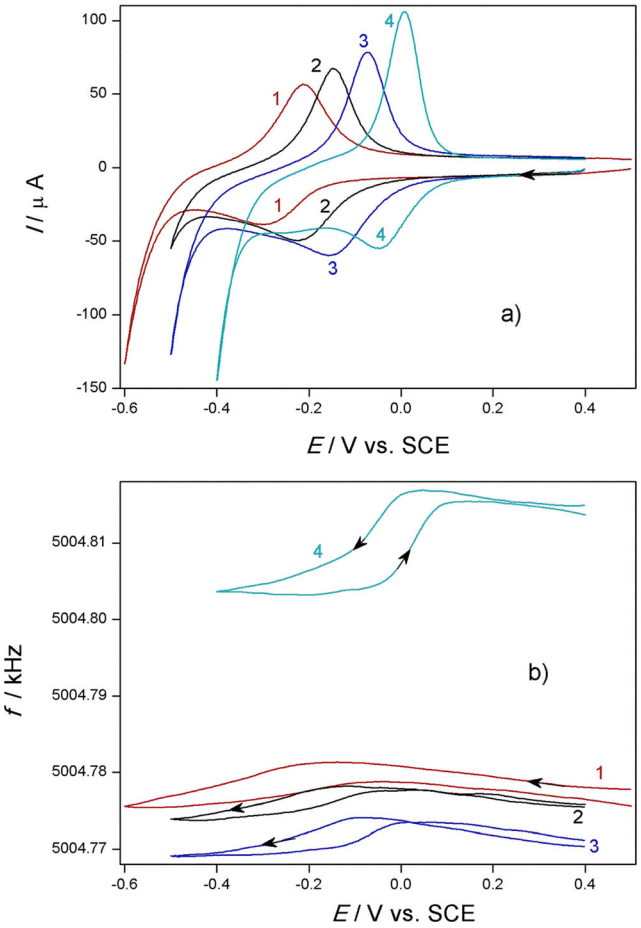

Fig. 2 Cyclic voltammetric (**a**) and the simultaneously obtained EQCN frequency (**b**) responses for an Au| poly(CuPc) electrode in contact with electrolyte solutions of different pH values at constant 1 mol dm^{-3} ionic strength: 1 mol dm^{-3} perchloric acid (*1*), 0.1 mol dm^{-3} perchloric acid+0.9 mol dm^{-3} $NaClO_4$ (*2*), 0.01 mol dm^{-3} perchloric acid+0.99 mol dm^{-3} $NaClO_4$ (*3*), and 0.001 mol dm^{-3} perchloric acid+0.999 mol dm^{-3} $NaClO_4$ (*4*). Scan rate 20 mV s^{-1}

Results and discussion

The pH dependence of the cyclic voltammetric and EQCN responses

Acidic solutions

Figure 2 shows a series of cyclic voltammetric and the simultaneously detected EQCN responses for a poly(CuPc) layer in contact with aqueous perchlorate electrolytes between pH 0 and 3.

It is evident that H^+ ions participate in the redox process, since with increasing pH the voltammetric peaks shift into the direction of the more negative potentials by 65±10 mV/pH in the range of pH 1 and 3. However, between pH 0 and 1, 110± 10 mV/pH was obtained indicating a 2 H^+/1 e^- reaction. The data obtained, when 1 mol dm^{-3} perchloric acid was used, to some extent deviate from the data obtained between pH 1 and 3, albeit the voltammetric behavior is similar. The difference of the anodic and cathodic peak potentials is 80±10 mV for the latter three experiments while at pH 0 this value is 45± 10 mV. The beginning of the hydrogen evolution reaction shows the same pH dependence; therefore, we can conclude that the redox reaction of poly (CuPc) is basically a 1 H^+/1 e^- reaction in these potential and pH regions. The cyclic voltammograms are very similar to those obtained for conducting polymers, e.g., for polyaniline [32] inasmuch as the anodic and cathodic peaks are asymmetric and showing a hysteresis. The peak current (electrochemical activity) decreases with increasing pH values. The EQCN frequency change is also smaller at higher pH values than at pH 0; however, within the experimental error, those are more or less the same with a decreasing tendency between pH 1 and 3. The EQCN results obtained in acidic solutions (see also later) show that during the cathodic and anodic scans, mass increase and decrease occur, respectively. Above 0.2 V, the reversible, small frequency changes can be assigned to the effect of the double layer charging.

By using a more concentrated acid solution, 5 mol dm^{-3} H_2SO_4 (Hammett acidity constant, H_o=−2.28), the cyclic voltammograms drastically change; both the anodic and cathodic waves split into two waves (Fig. 3). In fact, a small wave at pH 0 can also be seen at more cathodic potentials;

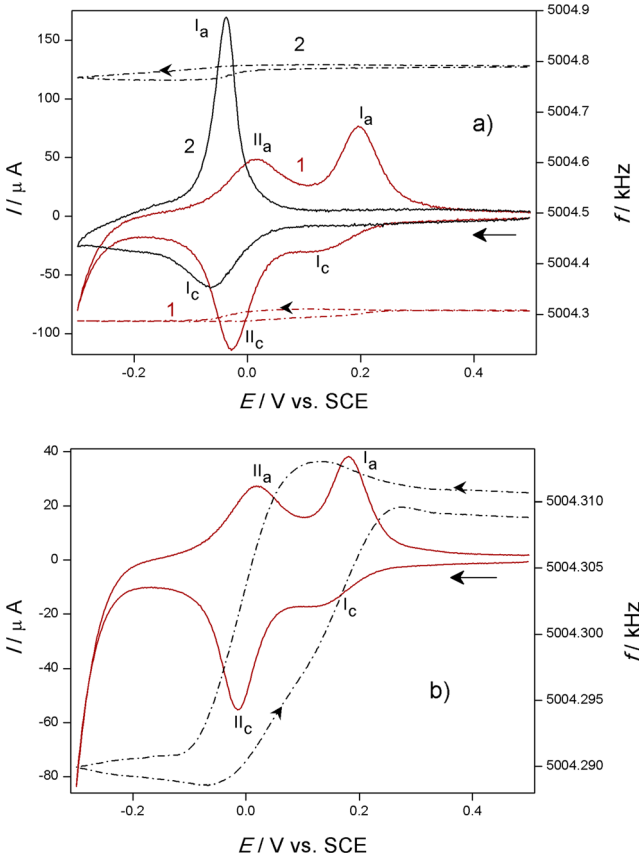

Fig. 3 Cyclic voltammetric (*continuous lines*) and the simultaneously obtained EQCN frequency (*dash-dotted lines*) responses for an Au| poly(CuPc) electrode in contact with 5 mol dm^{-3} H_2SO_4 (*1*) and 0.5 M H_2SO_4 (*2*) electrolyte solutions, respectively, at a scan rate of 20 mV s^{-1} (**a**) and in contact with 5 mol dm^{-3} H_2SO_4 electrolyte solution at a scan rate of 10 mV s^{-1} (**b**)

however, herein, it becomes the dominating one during the reduction (peak II_c). The pH dependence that was observed in the pH region from 0 to 1 changes again to ca. 60 mV/pH if the peaks at more positive potentials (peaks I) are considered and compared with the peak potentials observed in the case of less acidic solutions. It is reasonable to assume that peaks I belong to the unprotonated or partially protonated form, while peaks II are related to the doubly protonated form.

The response does not depend on the scan direction, and it can be seen that no oxidation occurs until 0.8 V (Fig. 4). The *M* values calculated by using Eq. (2) in the case of acidic solutions are summarized in Table 1.

In order to clarify the contribution of anions and cations to the ionic transport processes, the composition of the electrolyte was systematically varied. As an example for the effect of cations, the results obtained in the presence of LiCl in a high concentration are shown in Fig. 5. The shift of the voltammetric peaks as well as the beginning of the hydrogen evolution into the direction of higher potentials can be explained by the increased activity of the H^+ ions in concentrated electrolyte (acid + salt) solutions. The frequency change also

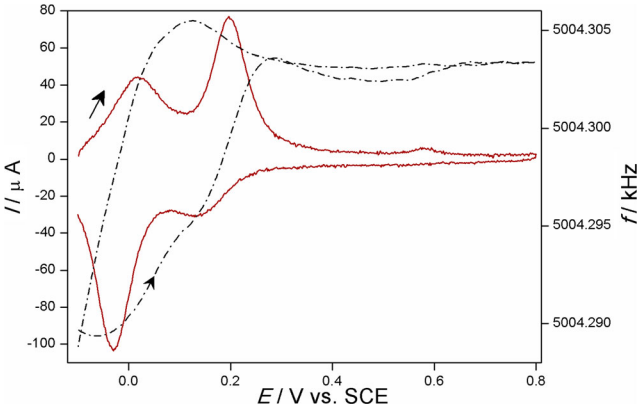

Fig. 4 Cyclic voltammetric (*continuous line*) and the simultaneously obtained EQCN frequency (*dash-dotted line*) responses for an Au| poly(CuPc) electrode in contact with 5 mol dm^{-3} H_2SO_4 electrolyte solution. Starting potential −0.1 V; scan rate 20 mV s^{-1}

increased in the LiCl-containing solution which can be related to the participation of the Li^+ ions and possibly that of the chloride ions in the charge-compensating processes.

The effect of anions is also evident. The cyclic voltammograms are similar in perchloric acid and hydrochloric acid. The charge under the voltammetric waves are the same. There is only a slight difference, i.e., in chloride-containing solutions, a more pronounced wave (II_c) appears at more cathodic potentials on the expense of the wave I_c. However, the mass change is higher in perchloric acid than that in HCl electrolyte (Fig. 6) indicating the incorporation of anions during the reduction.

Alkaline solutions

In alkaline media, the poly(CuPc) layer also shows a reversible redox behavior (Fig. 7). The shift of the peak potentials of

Table 1 Apparent molar masses (*M*/g mol^{-1}) of the exchanged species calculated for the respective redox transformations in acidic solutions

Solutions	Peak I_c	Peak I_a	Peak II_c	Peak II_a
$HClO_4 + NaClO_4$ *I*=1 mol dm^{-3}				
pH 0	(+) 51	(−) 52		
pH 1	(+) 12	(−) 16		
pH 2	(+) 11	(−) 16		
pH 3	(+) 20	(−) 18		
0.5 M H_2SO_4	(+) 80	(−) 91		
5 M H_2SO_4	(−) 32	(+) 79	(+) 88	(−) 69
1 M HCl	(+) 17	(−) 32		
1 M $HClO_4$[a]	(+) 54	(−) 44		

(+) and (−) symbols express the mass gain and mass loss, respectively, during the respective charge transfer process. The experimental scattering is ±15 % at a scan rate of 20 mV s^{-1}

[a] From other series of experiment than the date shown as pH 0

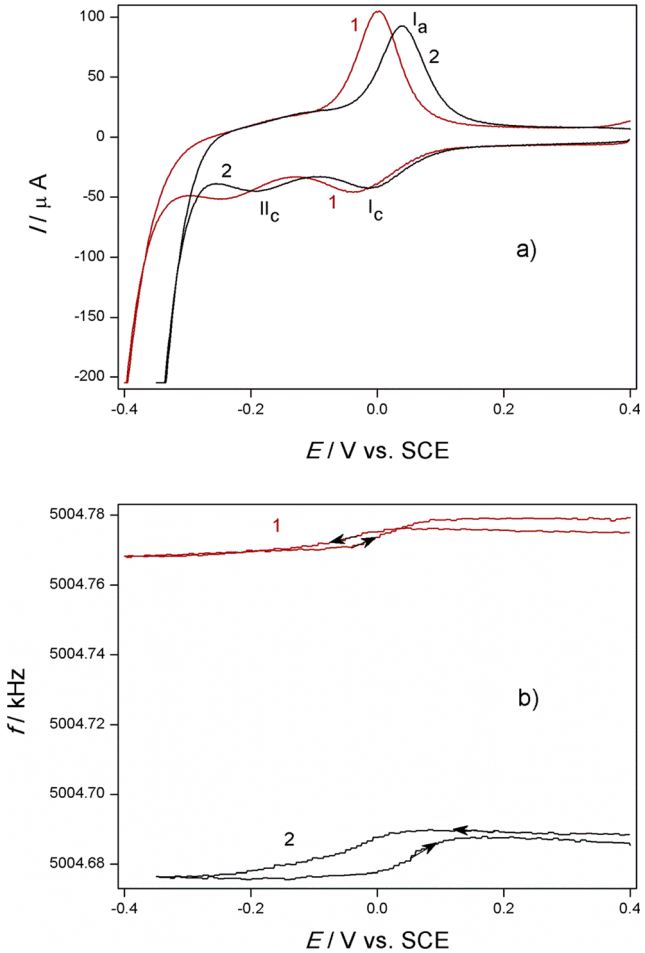

Fig. 5 Cyclic voltammetric (**a**) and the simultaneously obtained EQCN frequency (**b**) responses for an Au| poly(CuPc) electrode in contact with 1 mol dm^{-3} HCl (*1*) and 0.85 mol dm^{-3} HCl+3 mol dm^{-3} LiCl (*2*), respectively. Scan rate 20 mV s^{-1}

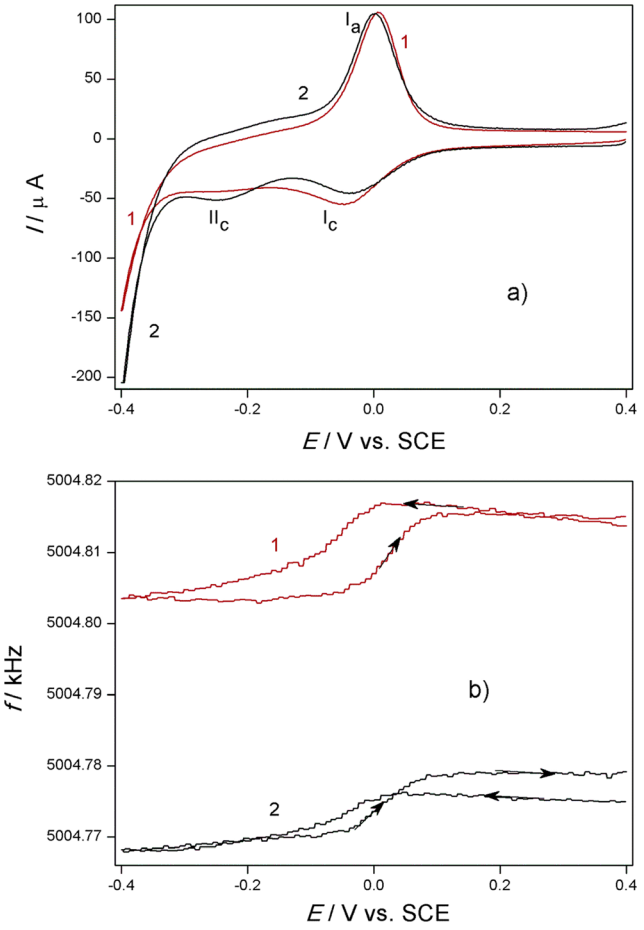

Fig. 6 Cyclic voltammetric (**a**) and the simultaneously obtained EQCN frequency (**b**) responses for an Au| poly(CuPc) electrode in contact with 1 mol dm^{-3} $HClO_4$ acid (*1*) and 1 mol dm^{-3} HCl (*2*), respectively. Scan rate 20 mV s^{-1}

the dominating redox reaction (peaks IV) as a function of pH corresponds to an 1 H^+/1 e^- reaction. Beside the main redox wave, a new, smaller wave appears (peaks III). However, the most remarkable feature is the change of the EQCN frequency response. During the cathodic scan in the region of peak III_c, a frequency increase (mass decrease) occurs. It is followed by a mass increase of similar magnitude at peak IV_c. During the reverse, anodic scan, the opposite phenomena can be observed. While the peak currents do not change substantially, the frequency change is getting higher with increasing pH values. In fact, a drastic increase can be detected at pH values higher than 12 which can be related to the deprotonation of a group having a pK_a value around pH 12. It should be mentioned that—albeit poly(CuPc) in alkaline media shows well-developed redox waves—the peak currents are somewhat smaller at the same scan rate for the same layer than that in acid media. On the other hand, the reversible frequency changes are much higher than that observed in acid media. The massogram (Fig. 7c) attests that the mass flux is in close relationship with the voltammetric current, i.e., the mass transfer is coupled to the charge transfer [33].

In order to get information about the nature of the exchanged species causing the frequency changes during potential cycling, the electrolyte solution was systematically changed also in alkaline media. Figure 8 shows the effect when at pH 12.38 (adjusted by KOH) the KCl electrolyte was replaced by CsCl. Beside Cs^+ ions, K^+ ions were also present from the KOH; however, there ratio was 21:1; therefore, in the case of cation transport, a higher change of the surface mass can be expected. Indeed, the mass change was larger when the electrolyte solution contained Cs^+ ions while the total charge under the voltammetric waves remain more or less the same. The *M* values calculated in the case of alkaline media are compiled in Table 2.

Based on the respective molar masses, a factor of 3.41 could be expected for the values obtained in the presence of Cs^+ and K^+ ions, respectively. This ratio found is less than 2; however, if water transport is also assumed, it can be explained by the higher hydration number of K^+ in comparison with that of Cs^+.

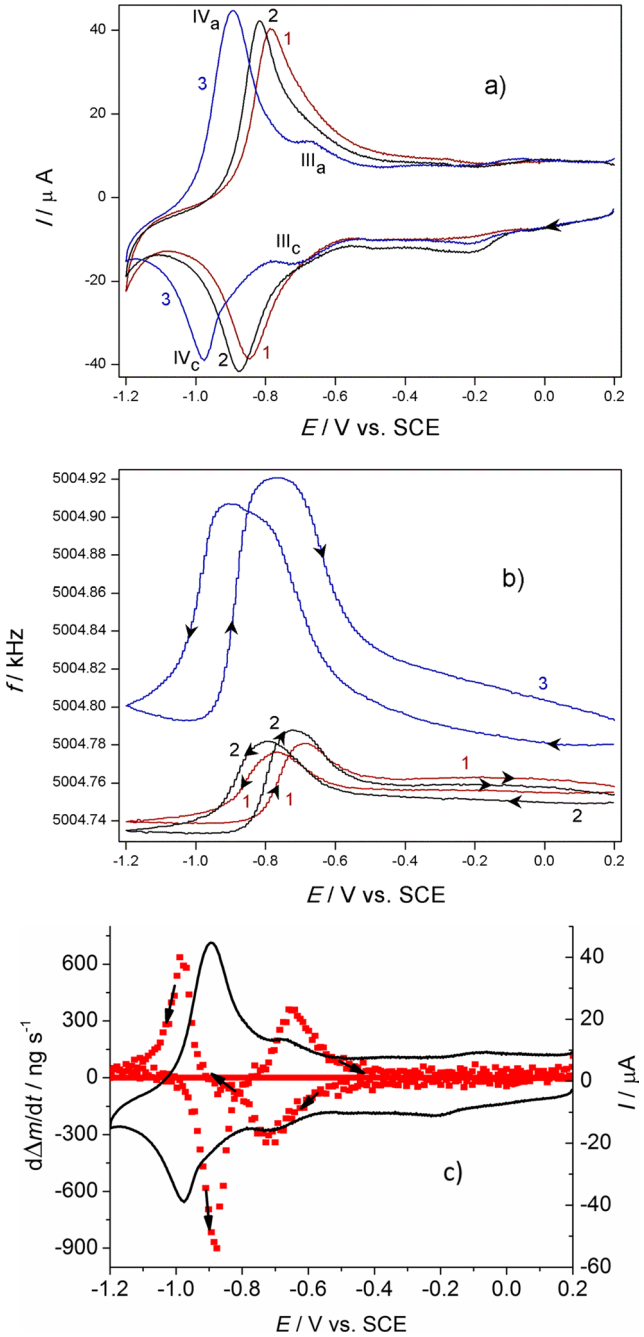

Fig. 7 Cyclic voltammetric (**a**) and the simultaneously obtained EQCN frequency (**b**) responses for an Au| poly(CuPc) electrode in contact with electrolyte solutions of 0.5 mol dm^{-3} KCl + suitable concentration of KOH for adjusting pH values. pH values are 11.0 (*1*), 11.4 (*2*), and 12.38 (*3*), respectively. The massogram [31] constructed by using the data of curve (*3*) (**c**). Scan rate 20 mV s^{-1}

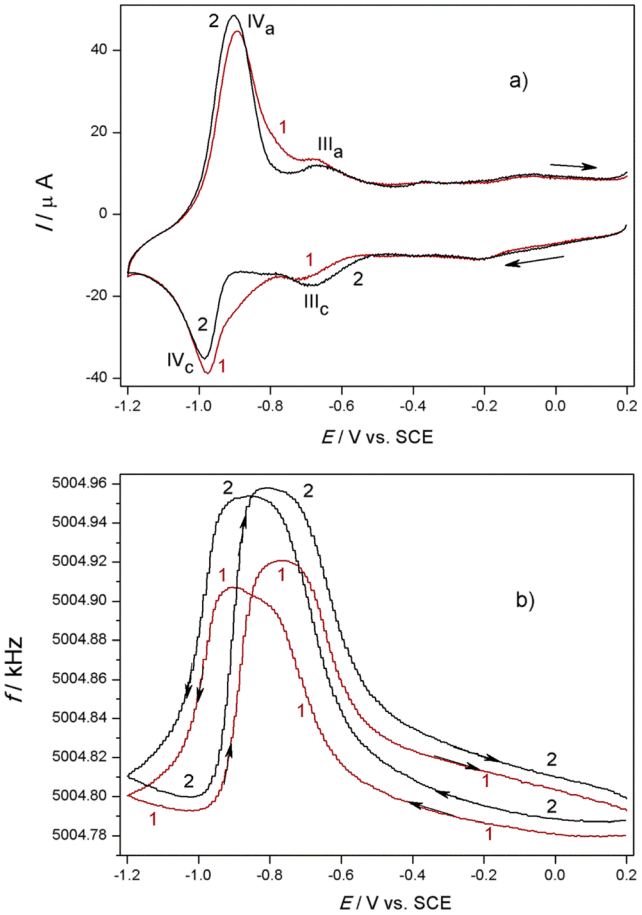

Fig. 8 Cyclic voltammetric (**a**) and the simultaneously obtained EQCN frequency (**b**) responses for an Au| poly(CuPc) electrode in contact with electrolyte solutions of pH 12.38 adjusted by KOH: 0.5 mol dm^{-3} KCl (*1*) and 0.5 mol dm^{-3} CsCl (*2*). Scan rate 20 mV s^{-1}

Neutral solutions

We tried to compare the voltammetric responses of poly(CuPc) in neutral, unbuffered media in order to get information on the cation effect. The shape of the voltammograms somewhat changed, but they were similar irrespective of the nature of the electrolyte (KCl or CsCl). However, the much higher EQCN frequency change in the presence of CsCl attests that the cation exchange plays a dominating role (Fig. 9). The split of the anodic voltammetric waves and the increase of the peak current at more anodic potentials, which was the

Table 2 Apparent molar masses (M/g mol^{-1}) of the exchanged species calculated for the respective redox transformations in alkaline media

Solutions	Peak III_c	Peak III_a	Peak IV_c	Peak IV_a
KOH + KCl				
pH 11	(−) 128	(+) 138	(+) 196	(−) 317
pH 11.4	(−) 156	(+) 237	(+) 258	(−) 479
pH 12.38	(−) 807	(+) 1238	(+) 712	(−) 957
KOH + CsCl				
pH 12.38	(−) 1165	(+) 1909	(+) 1050	(−) 1191

(+) and (−) symbols express the mass gain and mass loss, respectively, during the respective charge transfer reaction. The experimental scattering is ±20 % at a scan rate of 20 mV s^{-1}

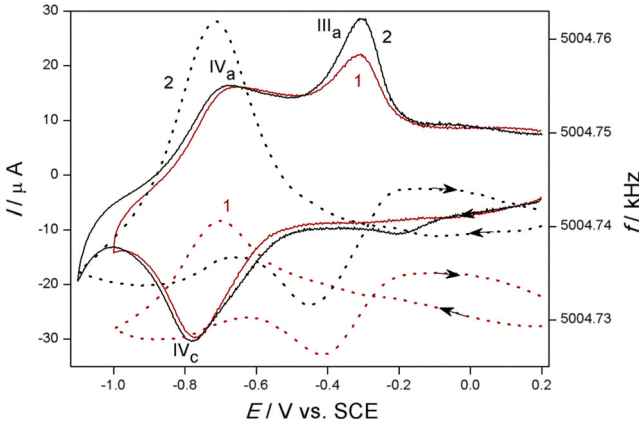

Fig. 9 Cyclic voltammetric (*continuous lines*) and the simultaneously obtained EQCN frequency (*dotted lines*) responses for an Au| poly(CuPc) electrode in contact with 0.5 mol dm^{-3} KCl (*1*) and 0.5 mol dm^{-3} CsCl (*2*), respectively. Scan rate 20 mV s^{-1}

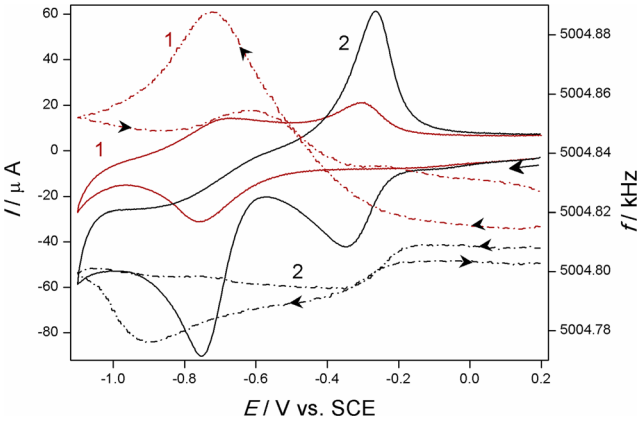

Fig. 11 Cyclic voltammetric (*continuous lines*) and the simultaneously obtained EQCN frequency (*dash-dotted line*) responses for an Au| poly(CuPc) electrode in contact with 0.5 mol dm^{-3} $NaClO_4$ (*2*). Scan rate 20 mV s^{-1}. Prehistory of the layer: the electrode had been soaked and cycled in pH 12 electrolyte (*1*) and 0.2 mol dm^{-3} $HClO_4$ (*2*), respectively. Then both electrodes were rinsed with distilled water and then with the solutions used in this experiment

smaller one in alkaline solution, may be related to the change of the pH in the vicinity of the layer due to protonation/deprotonation reactions accompanying the redox transformations. A closer inspection of the EQCN curve also reveals that during the cathodic scan, the frequency response is similar to that observed in alkaline media; however, especially in the region of peak III$_a$, the mass decrease resembles the change observed in acidic media, i.e., a frequency increase occurs.

We realized that in neutral media, especially the EQCN, responses strongly depend on the prehistory of the layer. When the layer had been investigated in acid and alkaline media, respectively, the EQCN responses were similar to those observed in the media used previously. This behavior prevails disregarding the intense rinsing and long time soaking in the neutral media before the experiments in neutral solutions, see also Figs. 10 and 11.

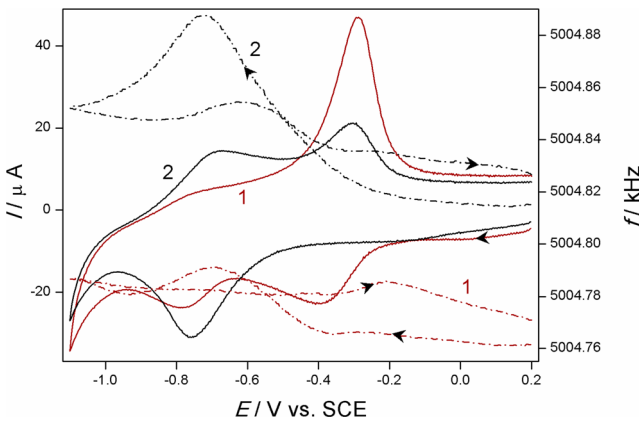

Fig. 10 Cyclic voltammetric (*continuous lines*) and the simultaneously obtained EQCN frequency (*dash-dotted lines*) responses for an Au| poly(CuPc) electrode in contact with 0.5 mol dm^{-3} NaCl (*1*) and 0.5 mol dm^{-3} $NaClO_4$ (*2*), respectively. Scan rate 20 mV s^{-1}. Prehistory of the layer: the electrode had been cycled in pH 12 electrolyte then rinsed with distilled water and then with the solutions used in this experiment

In neutral solutions, the EQCN frequency changes are higher in the presence of ClO_4^- ions than in Cl^--containing solutions if the same cation is used (Fig. 10). The *M* values obtained are summarized in Table 3.

In order to get information on the kinetics of the processes, scan rate dependence of the cyclic EQCN response has also been studied (see Supplementary Figures 1 and 2). According to the scan rate dependence of the peak currents, the waves observed are surface ones, at least the peak currents are proportional to the scan rate (*v*). The scan rate dependence of the EQCN response reveals that the redox transformations are accompanied with slow sorption/desorption processes. It is usually explained by the motion of the neutral solvent molecules, while the potential-driven migration of ions is fast. It should be mentioned that the uptake of a large amount of solvent can cause a substantial change of the structure of the microparticles. Phase transitions are also accompanied with extensive swelling-deswelling of the surface layer, while the stress arising in the surface layer can affect the EQCN

Table 3 Apparent molar masses (*M*/g mol^{-1}) of the exchanged species calculated for the respective redox transformations in neutral solutions

Solutions	Peak III$_c$	Peak III$_a$	Peak IV$_c$	Peak IV$_a$
pH 7				
0.5 M NaCl	(−) 154	(−) 37	(−) 80	(−) 37
0.5 M $NaClO_4$	(−) 541	(−) 151	(+) 248	(−) 133
0.5 M KCl	(−) 85	(+) 121	(+) 88	(+) 106
0.5 M CsCl	(−) 219	(+) 106	(+) 184	(+) 121

(+) and (−) symbols express the mass gain and mass loss, respectively, during the respective charge transfer reaction. The experimental scattering is ±20 % at a scan rate of 20 mV s^{-1}

response substantially [15, 28, 29, 34–38]. The scan rate dependence of the mass change is more pronounced in alkaline media as it is expected, since in this case the very high M values calculated can be related to structural changes and dehydration/hydration of the layer. Furthermore, in pure acid media, the dominating ionic transport process occurs via the motion of the H_3O^+ ions which is higher than that of other ions in aqueous solutions. The high mobility also prevails for OH^- ions in alkaline media. At pH 7, a transition from the surface to the diffusional behavior has been observed at higher scan rates, attesting the importance of the fast motion of the above-mentioned ions.

Scheme of the redox transformations

Acidic electrolytes

In order to give a reasonable scheme of the redox transformations, we have to take into account both the mass changes and the pH dependence of the voltammetric peaks observed. For the sake of simplicity, poly(CuPc) will be abbreviated as CuPc in the equations below. It can be assumed the protonation of bridging nitrogen atoms of the pyrrole part of the isoindole rings, and perhaps that of the nitrogen of the isoindole ring, may affect the properties and redox responses of the whole conjugated system. It is generally assumed that the central Cu^{2+} ions do not participate in the redox reaction [6, 8, 10].

The following facts have to be considered:

First, in the pH range from 0 to 3, only a single pair of waves can be observed; the shift is ca. −60 mV/pH. In more concentrated acid solutions, two pairs of waves appear, one of those related to the peaks observed in less acidic solutions since the above-mentioned potential shift as a function of pH prevails. In fact, the −60 mV/pH dependence is preserved in the whole pH range for the one-electron reduction even in alkaline solutions.

Based on spectroscopic evidences, the protonation of one or more bridging imine groups depending on the acidity of the contacting solution has been proposed. At high concentrations of strong acids, the protonation of more and more –C═NH–C groups is expected [22, 25–27]. The protonation of the nitrogen of the isoindole cannot be entirely excluded, either; however, it occurs only at very high concentrations of strong acids and at elevated temperatures. It eventually leads to the loss of the central Cu^{2+} ions [25]. In the case of protonation, to maintain the electroneutrality, anions enter the layer. The participation of water molecules can also be considered due to the change of the hydration of different reduced and protonated forms, and it is possible that water molecules as ligands can form a $(H_2O)_2$ $Cu^{2+}Pc^{2-}$ complex with CuPc as it has been proven for other metal phthalocyanines, e.g., $Fe^{2+}Pc^{2-}$ [15, 39].

Therefore, we consider the following protonation equilibria in acidic solutions:

$$Cu^{2+}Pc^{2-}(s) + 2H^+(aq) + 2A^-(aq) \rightleftarrows Cu^{2+}Pc^{2-}(H^+)_2(A^-)_2(s) \quad (3)$$

$$Cu^{2+}Pc^{2-}(s) + H^+(aq) + A^-(aq) \rightleftarrows Cu^{2+}Pc^{2-}H^+A^-(s) \quad (4)$$

Albeit usually monoprotonated and diprotonated forms have been considered [22], the existence of the protonation of all extracyclic N-atoms has also been suggested [27]. Protonation equilibria certainly exist in the case of the reduced forms:

$$Cu^{2+}Pc^{3-}H^+M^+A^-(s) + H^+(aq) + A^-(aq) \rightleftarrows Cu^{2+}Pc^{3-}M^+(H^+)_2(A^-)_2(s) \quad (5)$$

$$Cu^{2+}Pc^{3-}M^+(s) + H^+(aq) + A^-(aq) \rightleftarrows Cu^{2+}Pc^{3-}M^+H^+A^-(s) \quad (6)$$

In these equations, A^-═ClO_4^-, HSO_4^-, Cl^-, and M^+═Na^+, K^+, Cs^+ are used in our experiments. It can also be assumed that pK_a of the parent compound is higher than that of the reduced form; therefore, there is a pH interval when the original (unreduced) form is not protonated while the single reduced form is still protonated as in the case of leucoemeraldine and emeraldine forms of polyaniline [32, 40].

Second, the reaction scheme is obviously rather complex, the reactions are pH dependent. The ionic exchange processes during the redox transformations involve the sorption and desorption of H^+ ions and other cations as well as anions. Water molecules also contribute to the mass changes depending on the hydration of ions and the poly(CuPc) in its actual redox state, respectively. Indeed, it was observed that the mass changes depend on the nature of both anions and cations. However, in the course of both the first and the second reduction steps, the mass of the exchanged species, that can be calculated from the EQCN frequency change and the charge consumed, does not equal to the molar mass of the cation or the anion used in the experiments. On the other hand, in the presence of perchlorate or sulfate ions, higher mass change was observed than in chloride ion containing media, and similarly Cs^+ ions caused a higher mass change than Na^+ or K^+ ions during the given redox process. This observation can be

assigned to the transport of the solvent molecules (in some cases counterflux) as well as the simultaneous transport of cations and anions. We have to emphasize again that the requirements of the use of Sauerbrey equation for the calculation of the mass change were not met, either. Nevertheless, the *M* values calculated are reasonable, and at least the ratio of those obtained in the presence of different cations and anions, respectively, can be considered as reliable data.

Third, an explanation of the dependence of the mass change as a function of the nature of the anion (Figs. 2, 3, and 6, Table 1) has to be given, keeping in mind the protonation equilibria in acidic media.

During reduction, an incorporation of cations is expected in the simplest case, i.e.,

$$Cu^{2+}Pc^{2-}(s) + M^{+}(aq) + e^{-} \rightleftarrows Cu^{2+}Pc^{3-}M^{+}(s) \quad (7)$$

or

$$Cu^{2+}Pc^{2-}(s) + H^{+}(aq) + e^{-} \rightleftarrows Cu^{2+}Pc^{3-}H^{+}(s) \quad (8)$$

and

$$Cu^{2+}Pc^{2-}(s) + 2H^{+}(aq) + A^{-}(aq) + e^{-} \rightleftarrows Cu^{2+}Pc^{3-}(H^{+})_2A^{-}(s) \quad (9)$$

(Note that in the pH range between 0 and 1, a value close to 120 mV/pH was obtained.)

However, at low pH values, both the unreduced compound and the reduced one can be protonated, or depending on the pK_a values, the unreduced form is unprotonated while the reduced form is still protonated. Therefore, the following reaction should also be considered:

$$Cu^{2+}Pc^{2-}(s) + M^{+}(aq) + H^{+}(aq) + A^{-}(aq) + e^{-} \rightleftarrows Cu^{2+}Pc^{3-}M^{+}H^{+}A^{-}(s) \quad (10)$$

(Note that 60 mV/pH dependence was found that in the pH range between 1 and 3.)

In pure acidic solutions, both reactions (8) and (9) can occur simultaneously. By Eqs. (9) and (10), we can explain the higher mass change and the higher *M* values in the presence of perchlorate ions and sulfate ions in comparison with that of chloride ions (Table 1). It is reasonable to assume that these resultant *M* values are originated from two effects; redox reactions described by equations above that occur simultaneously, Eqs. (8) and (9) are operative in pure acid media and Eqs. (7) and (10) are valid when Na^+ ions are also present. A flux or counterflux of water molecules can also be responsible for the observed *M* values. If our assumption is true, the *M* values should decrease with increasing pH when Na^+ ions are also present, the participation of anions becomes smaller, and Eq. (7) will be the dominating process (Fig. 1). Indeed, it is the case since in the range of pH 1 and 3, the *M* value decreases to 16±5 g mol^{-1} which is close to the molar mass of the Na^+ ions. It indicates that reaction (7) starts to become the dominating reaction.

Below pH 0 (5 mol dm^{-3} H_2SO_4), we consider the existence of multiple protonated forms. Therefore, the possible reactions are as follows:

$$Cu^{2+}Pc^{2-}H^{+}A^{-}(s) + H^{+}(aq) + e^{-} \rightleftarrows Cu^{2+}Pc^{3-}(H^{+})_2A^{-}(s) \quad (11)$$

Note that in the region of the first reduction peak (peak I_c of Figs. 3 and 4), even a small mass decrease with *M*=32±10 can be observed that is followed by the mass increase (*M*=88±10).

$$Cu^{2+}Pc^{2-}(H^{+})_2(A^{-})_2(s) + 2H^{+}(aq) + A^{-}(aq) + e^{-} \rightleftarrows Cu^{2+}Pc^{3-}(H^{+})_4(A^{-})_3(s) \quad (12)$$

During the reoxidation in the first step at about 0 V, a mass decrease (*M*=78±10) occurs, i.e., H^+ ions and anions leave the film according to Eq. (13):

$$Cu^{2+}Pc^{3-}(H^{+})_4(A^{-})_3(s) \rightleftarrows Cu^{2+}Pc^{2-}(H^{+})_2(A^{-})_2(s) + 2H^{+}(aq) + A^{-}(aq) + e^{-} \quad (13)$$

It continues also in the potential region of the second anodic peak which can be related to the anodic reaction:

$$Cu^{2+}Pc^{3-}(H^{+})_3(A^{-})_2(s) \rightleftarrows Cu^{2+}Pc^{2-}H^{+}A^{-}(s) + 2H^{+}(aq) + A^{-}(aq) + e^{-} \quad (14)$$

Of course, the reaction mechanism is obviously more complicated, the sequence of the electron transfer and protonation/deprotonation reactions (ECE mechanism) can affect the responses substantially. We may also consider that the anions form axial ligand complexes with the central Cu^{2+} ions or anions can act as bridging ligand complexes between two Cu^{2+} ions [41–43]. By the help of this concept, the differences concerning the EQCN responses in the presence of different

anions, e.g., chloride, perchlorate, and sulfate, can be understood. Therefore, we can suggest also the reactions as follows:

$$\left[Cu^{2+}Pc^{2-}A^{-}\right]H^{+}(s) + H^{+}(aq) + e^{-} \rightleftarrows \left[Cu^{2+}Pc^{3-}A^{-}\right](H^{+})_2(s) \quad (15)$$

or

$$\left[Cu^{2+}Pc^{2-}A^{-}\right]Na^{+}(s) + H^{+}(aq) + e^{-} \rightleftarrows \left[Cu^{2+}Pc^{3-}A^{-}\right]NaH^{+}(s) \quad (16)$$

or

$$\left[Cu^{2+}Pc^{2-}A^{-}\right]Na^{+}(s) + Na^{+}(aq) + e^{-} \rightleftarrows \left[Cu^{2+}Pc^{3-}A^{-}\right](Na^{+})_2(s) \quad (17)$$

The ([]) brackets symbolize the complex, while the cations are considered as counterions.

Alkaline electrolytes

In alkaline solutions, two pairs of waves appear in the cyclic voltammograms (Figs. 7 and 8) which could be related to the Pc^{2-}/Pc^{3-} and Pc^{3-}/Pc^{4-} redox transformations [10, 39]. The EQCN frequency change is also reversible, however, more complicated than that obtained in acidic media. In the course of reduction at the peaks appearing at less negative potentials (peak III_c), a mass decrease occurs which is followed by a mass increase at the peak of the more negative potentials (peak IV_c). The frequency changes are very large, and consequently the molar masses that can be calculated for the exchanged species are also very high. The high *M* values calculated from the EQCN results can be related to structural changes. Dimerization or aggregation has already been reported in the case of phthalocyanines [10, 21, 22, 39].

When a structural change or a phase transition occurs, it is usually accompanied by the loss of water from the layer [34–38]. In our case, the water molecules can originate from either hydrate water or ligands.

Somewhat surprisingly, there is still a potential shift as a function of pH which equals to 70±10 mV/pH for both waves between pH 11 and 11.4, and 70±10 and 90±10 mV/pH for the peaks III_c and IV_c, respectively, above pH 11.4. It means that H^+ ions (or OH^- ions and water molecules) are still involved in the redox reactions.

The participation of cations should be considered because in the presence of Cs^+ ions, a higher mass change can be observed than in K^+-containing electrolyte (Fig. 8). For instance, it may mean that at peak III_c the Cs^+ ions replace more water molecules in the layer, while at peak IV_c the higher molar mass is responsible for the higher mass change. For the description of the pH dependence, the formation of OH^- ions has to be considered. We may consider the reduction of the water molecules belonging to the CuPc units. Alternatively, it is a reasonable assumption that Cu^{2+}-$(OH^-)_2$ axial ligands are formed in alkaline media, and during the reduction their removal occurs [41–43]. Furthermore, the formation of a mixed valence dimer can also be taken account. The fast protonation after the electron transfer is also possible.

Therefore, we may assume the following equations considering two consecutive redox reactions resulting in the formation of Pc^{3-} and Pc^{4-} species, respectively. These reaction sequences can explain both the pH dependence of the peak potentials and the mass changes simultaneously.

Scheme 1 electrochemical-chemical (EC) mechanism: electron transfer is followed with fast protonation and loss of OH^- ions in the first reduction step

$$Cu^{2+}Pc^{2-}(H_2O)_x(s) + e^{-} \rightleftarrows Cu^{2+}Pc^{3-}H^{+}(H_2O)_{x-y}(s) + OH^{-}(aq) + yH_2O(aq) \quad (18)$$

Instead of $Cu^{2+}Pc^{3-}H^+$, it would be better to write CuPcH as it is the usual way in organic electrochemistry; however, keeping the ionic form, the occurring event is more visible. It can explain both the pH dependence and the mass loss at peak III_c. However, the effect of cations and anions cannot be elucidated by this scheme, and the description of the mass increase in the course of the further reduction becomes also problematic.

Scheme 2 removal of axial ligands during reduction

If we assume the existence of axial ligands Cu^{2+}-$(OH^-)_2$ formed in alkaline media and their removal during the reduction, the effect of cations can also be elucidated.

Therefore, the first reduction step is as follows:

$$\left[Cu^{2+}Pc^{2-}(OH^{-})_2\right](M^{+})_2(H_2O)_x(s) + e^{-} \rightleftarrows \left[Cu^{2+}Pc^{3-}(OH^{-})\right](M^{+})_2(H_2O)_{x-y}(s) + OH^{-}(aq) + yH_2O(aq) \quad (19)$$

The ([]) brackets symbolize the complex, while the cations are considered as counterions and the water molecules may

belong to the complex or they are present as hydrate water molecules.

During the second reduction step,

$$\left[Cu^{2+}Pc^{3-}(OH^-)\right](H_2O)_{x-y}(M^+)_2(s) + M^+(aq) + X^-(aq) + e^- + zH_2O(aq) \rightleftarrows \left[Cu^{2+}Pc^{4-}\right]X^-(M^+)_3(H_2O)_{x-y+z}(s) + OH^-(aq) \quad (20)$$

cations and anions and possible water molecules enter the layer. Therefore, all effects, i.e., pH dependence, mass increase, role of the ions, and even scan rate dependence by the water transport, can reasonably be explained.

Scheme 3 dimerization concept

$$\left[Cu^{2+}Pc^{2-}(OH^-)_2\right](M^+)_2(H_2O)_x(s) + \left[Cu^{2+}Pc^{3-}(OH^-)\right](M^+)_2(H_2O)_x(s) \rightleftarrows \left[Cu^{2+}Pc^{2-}(OH^-)_2\right] - \left[Cu^{2+}Pc^{3-}(OH^-)\right](M^+)_4(H_2O)_{2x-y}(s) + yH_2O(aq) \quad (21)$$

The loss of high amount of water is most likely due to the dimerization. In this case, the further oxidation is as follows:

$$\left[Cu^{2+}Pc^{2-}(OH^-)_2\right] - \left[Cu^{2+}Pc^{3-}(OH^-)\right](M^+)_4(H_2O)_{2x-y}(s) + 3M^+(aq) + 3X^-(aq) + 3e^- + zH_2O(aq) \rightleftarrows \left[Cu^{2+}Pc^{4-}\right]_2(X^-)_3(M^+)_7(H_2O)_{2x-y+z}(s) + 3OH^-(aq) \quad (22)$$

Nevertheless, it is most likely that these reactions have a more complex mechanism in that several charge transfer and chemical steps are involved.

The results of the electrochemical nanogravimetry provided a new insight into the redox transformations and the nature of the accompanying ionic and solvent transport processes of the poly(CuPc) electrode. However, further studies are needed for the elucidation of the complex reaction mechanism.

Conclusions

The study of the potential-dependent ionic and solvent exchange processes by EQCN revealed the rather complex mechanism of the redox transformations of the poly(copper phthalocyanine) microparticles attached to gold surface in contact with aqueous solutions. The redox reactions belong to the reduction and reoxidation of the Pc ring. The pH dependence of the peak potentials indicates the participation of H^+ ions in the redox reactions in a 1 H^+/1 e^- ratio in acidic and neutral solutions and the formation of 1 OH^- ion/1 e^- in basic electrolytes. In acidic solutions, the protonation of the phthalocyanine strongly influences the mass changes. In alkaline solutions, dimerization occurs causing a change of the structure and dehydration/hydration of the layer. It manifests itself in the high apparent molar mass values obtained.

The poly(CuPc) layer is stable both in acidic and alkaline solutions during the reversible reduction and reoxidation processes. No oxidation of the poly(CuPc) sample occurs until 0.8 V vs. SCE in acidic solutions and 0.4 V vs. SCE in alkaline solutions, respectively. The reaction rates show a minimum value at neutral pH.

The relatively slow motion of solvent molecules introduces a scan rate dependence regarding the mass change during potential cycling which is more pronounced in alkaline media where the water transport plays an important role in the mechanism of the electrode processes.

Reaction schemes have been suggested taking into account the protonation steps in acidic media and the removal of the OH^- axial ligands in the course of reduction in alkaline solutions.

In acidic media above pH 0, the product of the first reduction step is $Cu^{2+}Pc^{3-}$ $(H^+)_2A^-$ or $Cu^{2+}Pc^{3-}$ $M^+H^+A^-$, while below pH 0 the formation of $Cu^{2+}Pc^{3-}$ $(H^+)_2A^-$ and $Cu^{2+}Pc^{3-}$ $(H^+)_4$ $(A^-)_3$ occurs in two steps. We may also consider that the anions form axial ligand complexes with the central Cu^{2+} ions or anions can act as bridging ligand complexes between two Cu^{2+} ions [41–43]. By the help of this concept, the differences in the cyclic voltammetric and mass responses in the presence of different anions can be related to the existence of axial or bridging ligands.

It is proposed that under alkaline conditions axial ligands Cu^{2+}-$(OH^-)_2$ are formed. Considering their removal during the reduction,

$$\left[Cu^{2+}Pc^{2-}(OH^-)_2\right](M^+)_2(H_2O)_x(s) + e^- \rightleftarrows \left[Cu^{2+}Pc^{3-}(OH^-)\right](M^+)_2(H_2O)_{x-y}(s) + OH^-(aq) + yH_2O(aq) \left[Cu^{2+}Pc^{3-}(OH^-)\right](H_2O)_{x-y}(M^+)_2(s) + M^+(aq) + X^-(aq) + e^- + zH_2O(aq) \rightleftarrows \left[Cu^{2+}Pc^{4-}\right]X^-(M^+)_3(H_2O)_{x-y+z}(s) + OH^-(aq)$$

both the pH dependence of the peak potentials and the mass changes can be elucidated regarding both reduction steps. It is

also assumed that the high mass loss occurs during a dimerization reaction, and accordingly the dehydration can be described as follows:

$$\left[Cu^{2+}Pc^{2-}(OH^-)_2\right](M^+)_2(H_2O)_x(s) + \left[Cu^{2+}Pc^{3-}(OH^-)\right](M^+)_2(H_2O)_x(s) \rightleftarrows \left[Cu^{2+}Pc^{2-}(OH^-)_2\right] - \left[Cu^{2+}Pc^{3-}(OH^-)\right](M^+)_4(H_2O)_{2x-y}(s) + yH_2O(aq)$$

In this case, the further reduction step is the reduction of the mixed valence dimer:

$$\left[Cu^{2+}Pc^{2-}(OH^-)_2\right] - \left[Cu^{2+}Pc^{3-}(OH^-)\right](M^+)_4(H_2O)_{2x-y}(s) + 3M^+(aq) + 3X^-(aq) + 3e^- + zH_2O(aq) \rightleftarrows \left[Cu^{2+}Pc^{4-}\right]_2(X^-)_3(M^+)_7(H_2O)_{2x-y+z}(s) + 3OH^-(aq)$$

The behavior of poly(copper phthalocyanine)—which is a conjugated system—resembles that of other conducting polymers.

Acknowledgments A financial support of the National Scientific Research Fund (OTKA K100149) is gratefully acknowledged.

References

1. Leznoff CC, Lever APB (eds) Phthalocyanines: properties and applications. VCH Publ., New York, 1989–1996, vols. 1–4
2. Alpatova NM, Ovsyannikova EV (2011) Electropolymerization of phthalocyanines. In: Cosnier S, Karyakin A (eds) Electropolymerization. Wiley-VCH, Weinheim, pp 111–132
3. Sakamoto K, Ohno-Okumura E (2009) Syntheses and functional properties of phthalocyanines. Materials 2:1127–1179
4. Jansen R, Beck F (1994) Electrochemical characterization and transformation of redox states at the surface of metallophthalocyanines. Electrochim Acta 39:921–931
5. Komorsky-Lovrić S (1995) Voltammetry of microcrystals of cobalt and manganese phthalocyanines. J Electroanal Chem 397(1–2):211–215
6. Jiang J, Kucernak AR (2001) The electrochemistry of platinum phthalocyanine microcrystals. IV. Temperature dependence of the electrochemical behaviour in non-aqueous solution. Electrochim Acta 46:3445–3456
7. Brown RJC, Brett DJL, Kucernak ARJ (2009) An electrochemical quartz crystal microbalance study of platinum phthalocyanine thin films. J Electroanal Chem 633:339–346
8. Caro CA, Zagal JH, Bedioui F (2003) Electrocatalytic activity of substituted metallophthalocyanines adsorbed on vitreous carbon electrode for nitric oxide oxidation. J Electrochem Soc 150:E95–E103
9. Gaffo L, Goncalves D, Faria RC, Moreira WC, Oliveira ON Jr (2005) Spectroscopic, electrochemical, and microgravimetric studies on palladium phthalocyanine film. J Porphyrins Phthalocyanines 9(1): 16–21
10. Arici M, Arican D, Lütfi Ugur A, Erdogmus A, Koca A (2013) Electrochemical and spectroelectrochemical characterization of newly synthesized manganese, cobalt, iron and copper phthalocyanines. Electrochim Acta 87:554–566
11. Yamazaki S, Fujiwara N, Yasuda K (2010) A catalyst that uses a rhodium phthalocyanine for oxalic acid oxidation and its application to an oxalic acid sensor. Electrochim Acta 55:753–758
12. Akinbulu IA, Ozoemena KI, Nyokong T (2011) Formation, surface characterization, and electrocatalytic application of self-assembled monolayer films of tetra-substituted manganese, iron, and cobalt benzylthio phthalocyanine complexes. J Solid State Electrochem 15(10):2239–2251
13. Selvaraj C, Munichandraiah N, Scanlon LG (2012) Dilithium phthalocyanine as a catalyst for oxygen reduction in non-aqueous Li-O_2 cells. J Porphyrins Phthalocyanines 16:255–259
14. Nemes Á, Moore CE, Inzelt G (2013) Electrochemical and nanogravimetric studies of palladium phthalocyanine microcrystals. J Serb Chem Soc 78:2017–2037
15. Nemes Á, Inzelt G (2014) Electrochemical and nanogravimetric studies of iron phthalocyanine microparticles immobilized on gold in acidic and neutral media. J Solid State Electrochem 18:3327–3337
16. Reynolds JR, Pyo M, Qiu YJ (1994) Charge and ion transport in poly(pyrrole copper phthalocyanine tetrasulfonate) during redox switching. J Electrochem Soc 141:35–40
17. Sousa AL, Santos WJR, Luz RCS (2008) Amperometric sensor for nitrite based on copper tetrasulphonated phthalocyanine immobilized with poly-L-lysine film. Talanta 75:333–338
18. Acres GJK, Eley DD (1964) Activation of hydrogen by poly copper phthalocyanine. Trans Faraday Soc 60:1157–1169
19. Reis RM, Valim RB, Rocha RS, Lima AS, Castro PS, Bertotti M, Lanza MRV (2014) The use of copper and cobalt phthalocyanines as electrocatalysts for the oxygen reduction reaction in acid medium. Electrochim Acta 139:1–6
20. Fc M, Mascaro LH, Machado SAS, Brett CMA (2010) Direct electrochemical determination of glyphosate at copper phthalocyanine/multiwalled carbon nanotube film electrodes. Electroanalysis 22: 1586–1591
21. Meier H, Albrect W, Zimmerhackl E (1985) Photoconductivity of copper phthalocyanine. Polym Bull 13:43–50
22. Su JL, Xue MZ, Ma N, Sheng QR, Zhang Q, Liu YG (2009) Dissolution of copper phthalocyanine and fabrication its nanostructure film. Sci China Ser B Chem 52:911–915
23. Kreja L, Czerwinski W (1992) A study of iodine influence on the electrical properties of phthalocyanines and polyphthalocyanines of some metals. J Mater Sci Lett 11:538–540
24. Raïssi M, Vignau L, Ratier B (2014) Enhancing the short-circuit current, efficiency of inverted organic solar cells using tetra sulfonic copper phthalocyanine (TS-CuPc) as electron transporting layer. Org Electron Phys Mater Appl 15:913–919
25. Sokolova TN, Lomova TN, Klueva ME, Suslova EE, Mayzlish VE, Shaposhnikov GP (2000) Structure-stability relationships of phthalocyanine copper complexes. Molecules 5:775–785
26. Ogunsipe AO, Idowu MA, Ogunbayo TB, Akinbulu IA (2012) Protonation of some non-transition metal phthalocyanines-spectral and photophysicochemical consequences. J Porphyrins Phthalocyanines 16:885–894
27. Srivasta KP, Kumar A (2001) UV spectral studies in protonation of Cu-phthalocyanine and phthalocyanine in sulphuric acid-solvent. Asian J Chem 13:1539–1543
28. Inzelt G (2010) Electrochemical quartz crystal nanobalance. In: Scholz F (ed) Electroanalytical methods, vol 10, 2nd edn. Springer, Berlin, pp 257–270
29. Scholz F, Schröder U, Gulaboski R (2005) Electrochemistry of immobilized particles and droplets. Springer, Berlin, p 114

30. Scholz F, Gulaboski R, Caban K (2003) Electrochem Commun 5: 929–934
31. Scholz F, Gulaboski R (2005) ChemPhysChem 6:16–28
32. Inzelt G (2012) Conducting polymers—a new era in electrochemistry. In: Scholz F (ed) Monographs in electrochemistry, 2nd edn. Springer, Heidelberg Berlin
33. Snook GA, Bond AM, Fletcher S (2002) The use of massograms and voltammograms for distinguishing five basic combinations of charge transfer and mass transfer at electrode surface. J Electroanal Chem 526:1–9
34. Suárez MF, Bond AM, Compton RG (1999) Significance of redistribution reactions detected by in situ atomic force microscopy during early stages of fast scan rate redox cycling experiments at a solid 7,7, 8,8-tetracyanoquinodimethane-glassy carbon electrode-aqueous (electrolyte) interface. J Solid State Electrochem 4:24–33
35. Evans CD, Chambers JQ (1994) Electrochemical quartz crystal microbalance study of tetracyanoquinodimethane conducting salt electrodes. Chem Mater 6:454–460
36. Hepel M, Janusz W (2000) Study of leuco-methylene blue film growth and its reoxidation on sulphur-modified Au-EQCN electrode. Electrochim Acta 45(22–23):3785–3799
37. Puskás Z, Inzelt G (2004) Electrochemical microgravimetric study on microcrystalline particles of phenazine attached to gold electrodes. J Solid State Electrochem 8:828–841
38. Inzelt G, Róka A (2008) Electrochemical nanogravimetric studies of ruthenium(III)trichloride microcrystals. Isr J Chem 48:185–197
39. Kim S, Ohta T, Kwag G (2000) In situ structural investigation of iron phthalocyanine monolayer adsorbed on electrode surface by X-ray absorption fine structure. Bull Korean Chem Soc 21:588–594
40. Bácskai J, Kertész V, Inzelt G (1993) An electrochemical quartz crystal microbalance study of the influence of pH and solution composition on the electrochemical behaviour of poly(aniline) films. Electrochim Acta 38:393–397
41. Greenwood NN, Earnshaw A (1997) Chemistry of the elements, 2nd edn. Butterworth-Heinemann, UK, pp 1630–1631
42. Kadish KM, Van Caemelbecke E (2002) Electrochemistry of metalloporphyrins in nonaqueous media. In: Scholz F, Pickett CJ, Bard AJ, Stratmann M (eds) Encyclopedia of electrochemistry, vol 7b. Wiley-VCH, Weinheim, pp 992–1046
43. Rorabacher DB, Schroeder RR (2006) Electrochemistry of copper. In: Wilson GS, Bard AJ, Stratmann M (eds) Encyclopedia of electrochemistry, vol 9. Wiley-VCH, Weinheim, pp 175–227